

## Specific Heat Anomaly for a Layer Antiferromagnet

Y. M. Nie<sup>1</sup>, P. Y. Hsiao<sup>1</sup>, Y. F. Chiang<sup>1</sup> and T. K. Lee<sup>1,2</sup>

<sup>1</sup>*Institute of Physics, Academia Sinica, Taipei, Taiwan 115, R.O.C.*

<sup>2</sup>*National Center for Theoretical Sciences, P.O. Box 2-131, Hsinchu, Taiwan 300, R.O.C.*

(Received July 19, 2001)

The pronounced specific heat anomaly observed in cuprate oxide superconductors with Gd layers below the Néel temperature  $T_N$  is studied by using the modified spin-wave theory for an anisotropic layer antiferromagnetic system. The present work elucidates that the anomaly feature is mainly due to the large spin effect of the  $Gd^{3+}$ -ion. Our result agrees well with the experiments. In addition, the observed disappearance of the specific heat anomaly in the presence of a magnetic field is also obtained. The specific heat above  $T_N$  is calculated by using a high temperature expansion. The breakdown of the generalized modified spin-wave theory for the large-spin layer antiferromagnetic systems is explicitly demonstrated in the evaluation of the sublattice magnetization and correlation function.

PACS. 75.30.Ds – Spin Waves.

PACS. 75.40.-s – Critical-point effects, specific heats, short-range order.

PACS. 75.50.Ee – Antiferromagnetics.

### I. Introduction

An antiferromagnetic (AFM) phase transition occurs in the rare-earth (R) ion layers of high temperature cuprate oxide superconductors at a very low Néel temperature  $T_N$  [1-11]. So far it is believed that this AFM transition is not coupled with the superconducting Cu-O layers. Among the compounds studied, the ones with  $Gd^{3+}$ -ion layers show a pronounced anomaly below  $T_N$  in specific heat measurements [1-11]. Such an anomaly not only occurs in cuprate oxide superconductors, but also in other Gd alloys [12-15]. The entropy obtained by directly integrating the  $C = T \int T$  curve over the anomalous region is consistent with the magnetic mechanism scenario [1-15]. Furthermore, the anomaly is destroyed simultaneously, as the external magnetic field quenches the AFM ordering [11].

Blanco *et al.* [16] proposed a model with the amplitude-modulated exchange coupling to explain the specific heat anomaly in Gd alloys. Here we only consider the usual Heisenberg model with a layer structure to account for the specific heat anomaly of high temperature superconductors with Gd. Our results shows that the anomaly is mainly due to the large spin ( $S = 7/2$ ) of the  $Gd^{3+}$ -ion. At the AFM transition, only part of the spin degree of freedom is frozen. Quantum fluctuation of the remaining degrees of freedom contributes toward the specific heat anomaly. Our analysis not only produces values of  $T_N$  and an in-plane exchange coupling constant in good agreement with experiments [17], we also obtain a good estimate of the value of the inter-layer exchange coupling constant on the order of several Kelvin.

For a two-dimensional Heisenberg system, the modified spin-wave theory (MSWT) proposed by Takahashi [18] has been very successful. It predicts the long-range order at zero temperature with quite accurate sublattice magnetization. Liu [19] has modified this method and generalized it to layer systems. However, that author had not realized the breakdown of the theory near and above the Néel temperature. This has been pointed out by several groups in an approach similar to the MSWT [20-22]. These were attempts [23-26] to improve the MSWT or similar theories without success. Since the specific heat anomaly studied occurs at temperatures well below  $T_N$ , it is still appropriate to apply the MSWT. To estimate the specific heat above  $T_N$ , we use the high temperature expansion method. In the presence of a magnetic field, the MSWT has a non-Hermitian mean-field Hamiltonian. To avoid this non-Hermitian problem, we applied the large  $S$  expansion from the Holstein-Primakoff transformation to calculate the specific heat.

The present paper is organized as follows. In Sec. II., the formalism of the MSWT generalized for the layer system is shown. Results for the free energy, sublattice magnetization, correlation, and specific heat are presented. The breakdown of the theory near and above  $T_N$  is exhibited distinctly therein. In Sec. III. the formalism for the large  $S$  expansion as well as that of the high temperature expansion are illustrated. The comparison of the numerical results to the experimental measurements [11] in the presence of a magnetic field is depicted. Finally, a concise conclusion is made in Sec. IV.

## II. Modified spin-wave theory

### II-1. Formalism

The Heisenberg model Hamiltonian of the layer AFM in the form of a tetragonal lattice can be expressed as

$$H = \sum_{\langle i; j \rangle} J_{ij} \mathbf{S}_i \cdot \mathbf{S}_j; \quad (1)$$

$$[\hat{S}_i^\alpha; \hat{S}_j^\beta] = i \delta_{\alpha\beta} \delta_{ij} \epsilon_{\alpha\beta\gamma} \hat{S}_i^\gamma \quad (\alpha; \beta; \gamma = x; y; z); \quad (2)$$

$$\hat{S}_i^2 = S(S + 1);$$

where  $\langle i; j \rangle$  denotes the couple of the nearest-neighbor of the  $i$ -th site,  $J_{ij} = J$  ( $J_\gamma$ ) represents the intra-plane (inter-plane) exchange integral. The lattice is assumed to be bipartite and divided into A and B sublattices. On the sublattices A and B, the vacuum state is defined as  $S^z = S$  and  $S^z = j S$  respectively. Following Takahashi [18], the Dyson-Maleev transformation is used to transfer the spin operator into the boson-representation [27, 28].

$$S_m^x = a_m^y; \quad S_m^+ = (2S - a_m^y a_m) a_m; \quad S_m^z = S - a_m^y a_m; \quad m \in A; \quad (3)$$

$$S_n^x = j b_n; \quad S_n^+ = j b_n^y (2S - j b_n^y b_n); \quad S_n^z = j S + b_n^y b_n; \quad n \in B; \quad (4)$$

The commutation of the spin operator in Eq. (2) is consistent with the boson operator commutations.

$$[a_m; a_m^y] = \pm_{mm^y}; \quad [b_n; b_n^y] = \pm_{nn^y}; \quad (5)$$

$$[a_m; a_m^0] = [b_n; b_n^0] = [a_m^y; a_m^{0y}] = [b_n^y; b_n^{0y}] = 0; \quad (6)$$

$$[a_m^y; b_n] = [a_m; b_n^y] = [a_m^y; b_n^y] = [a_m^y; b_n^y] = [a_m; b_n] = 0; \quad (7)$$

The Hamiltonian (1) can be written as

$$H = \sum_i \frac{1}{2} (ZJ + Z_{\uparrow} J_{\uparrow}) N S^2 + \sum_{l; i \in 2A} \sum_{\pm} \mathbf{X} \cdot \mathbf{X} \cdot S (a_{li}^y a_{li} + b_{l; i \pm}^y b_{l; i \pm} + a_{li}^y b_{l; i \pm}^y + a_{li} b_{l; i \pm}) + \frac{1}{2} a_{li}^y (b_{l; i \pm}^y + a_{li})^2 b_{l; i \pm} + \sum_{l; i \in 2A} \sum_{\pm z} \mathbf{X} \cdot \mathbf{X} \cdot S (a_{li}^y a_{li} + b_{l; i \pm z}^y b_{l; i \pm z} + a_{li}^y b_{l; i \pm z}^y + a_{li} b_{l; i \pm z}) + \frac{1}{2} a_{li}^y (b_{l; i \pm z}^y + a_{li})^2 b_{l; i \pm z}; \quad (8)$$

where  $l$  denotes the  $l$ -th layer,  $\mathbf{X}(\pm z)$  denotes the nearest-neighbor lattice vectors parallel (perpendicular) to the plane.  $Z$  ( $Z_{\uparrow}$ ) is the intra-(inter-)plane coordination number, equal to 4 (2) in present work.

By means of the mean-field theory treatment, the  $k$ -space representation of the Hamiltonian derived from the Fourier transform is written as

$$H_{MF} = \sum_{\mathbf{k}} \frac{1}{2} (ZJ + Z_{\uparrow} J_{\uparrow}) N S^2 + \sum_{\mathbf{k}} \mathbf{X} \cdot \mathbf{X} \cdot \mathbf{P}_0 (ZJ \hat{A}_{\mathbf{k}} + Z_{\uparrow} J_{\uparrow} \hat{A}_{\uparrow \mathbf{k}}) (a_{\mathbf{k}}^y a_{\mathbf{k}} + b_{\mathbf{k}}^y b_{\mathbf{k}}) + \sum_{\mathbf{k}} \mathbf{X} \cdot \mathbf{X} \cdot \mathbf{P}_0 (ZJ \hat{A}_{\mathbf{k}} + Z_{\uparrow} J_{\uparrow} \hat{A}_{\uparrow \mathbf{k}}) (a_{\mathbf{k}}^y b_{\mathbf{k}}^y + a_{\mathbf{k}} b_{\mathbf{k}}); \quad (9)$$

where  $\mathbf{P}_0$  represents the summation over half of the first Brillouin zone.  $\hat{A}$  and  $\hat{A}_{\uparrow}$  are defined as

$$\hat{A} = \sum_i S_i (h b_{l; i \pm}^y b_{l; i \pm} + h a_{li} b_{l; i \pm}) = \sum_i S_i (h a_{li}^y a_{li} + h a_{li}^y b_{l; i \pm}^y); \quad (10)$$

$$\hat{A}_{\uparrow} = \sum_i S_i (h b_{l; i \pm z}^y b_{l; i \pm z} + h a_{li} b_{l; i \pm z}) = \sum_i S_i (h a_{li}^y a_{li} + h a_{li}^y b_{l; i \pm z}^y);$$

$\circ_{\mathbf{k}}$  and  $\circ_{\uparrow \mathbf{k}}$  are the intra- and inter-plane geometrical factor, respectively, defined as

$$\circ_{\mathbf{k}} = \frac{1}{Z} \sum_{\pm} \mathbf{X} \cdot e^{i\mathbf{k} \cdot \mathbf{X}_{\pm}}; \quad \circ_{\uparrow \mathbf{k}} = \frac{1}{Z_{\uparrow}} \sum_{\pm z} \mathbf{X} \cdot e^{i\mathbf{k} \cdot \mathbf{X}_{\pm z}}; \quad (11)$$

The Hamiltonian (9) can be diagonalized by the Bogoliubov transformation,

$$\begin{aligned} \alpha_{\mathbf{k}} &= \cosh \mu_{\mathbf{k}} a_{\mathbf{k}} - \sinh \mu_{\mathbf{k}} b_{\mathbf{k}}^y; \\ \beta_{\mathbf{k}}^y &= -\sinh \mu_{\mathbf{k}} a_{\mathbf{k}} + \cosh \mu_{\mathbf{k}} b_{\mathbf{k}}^y; \end{aligned} \quad (12)$$

Following reference [18] we use a chemical potential  $\mu$ , then the energy dispersion of the boson is obtained as

$$\epsilon_{\mathbf{k}} = \mu + \frac{1}{2} \left[ \epsilon_{\mathbf{k}}^2 + (\circ_{\mathbf{k}} + \circ_{\uparrow \mathbf{k}})^2 \right]; \quad (13)$$

where  $\rho = zJ\hat{A} + z\gamma J\hat{A}^{-1}$ ,  $\rho = zJ\hat{A}$ , and  $\gamma = z\gamma J\hat{A}$ .  $\langle S_i^z \rangle$  equals to the sublattice magnetization  $M$  for  $T > T_N$ , Eq. (3) and (4) give  $S_i = M = \langle a_m^\dagger a_m \rangle = \langle b_n^\dagger b_n \rangle$ . By virtue of the boson density matrix

$$\frac{1}{Z} = \exp \frac{1}{T} \sum_k \left( \epsilon_k y_k^\dagger + \epsilon_k^- y_k^- \right); \tag{14}$$

we can calculate

$$\begin{aligned} \langle a_{i\pm}^\dagger a_{i\pm} \rangle &= \langle b_{i\pm}^\dagger b_{i\pm} \rangle = f(r_i | r_{i\pm}); \\ \langle a_{i\pm}^\dagger b_{i\pm} \rangle &= \langle b_{i\pm}^\dagger a_{i\pm} \rangle = g(\pm); \\ \langle a_{i\pm}^\dagger b_{i\pm\pm} \rangle &= \langle b_{i\pm\pm}^\dagger a_{i\pm} \rangle = g_z(\pm_z); \\ f(0) &= \frac{2}{N} \sum_k \frac{1}{1 + (\epsilon_k + \gamma \epsilon_k^0)^2} \frac{\mu}{2} \coth(\epsilon_k = 2T); \\ g(\pm) &= \frac{2}{N} \sum_k \frac{\epsilon_k + \gamma \epsilon_k^0}{1 + (\epsilon_k + \gamma \epsilon_k^0)^2} \frac{\epsilon_k}{2} \coth(\epsilon_k = 2T); \\ g_z(\pm_z) &= \frac{2}{N} \sum_k \frac{\epsilon_k + \gamma \epsilon_k^0}{1 + (\epsilon_k + \gamma \epsilon_k^0)^2} \frac{\mu}{2} \coth(\epsilon_k = 2T); \end{aligned}$$

At a finite temperature, we have three self-consistent equations

$$S + \frac{1}{2} = M + f(0); \tag{15}$$

$$\frac{\rho}{zJ} = M + g(\pm); \tag{16}$$

$$\frac{\gamma \rho}{Jz\gamma} = M + g_z(\pm_z); \tag{17}$$

For  $\gamma = 1$ , Eqs. (15)-(17) coincide with the formalism for the isotropic three-dimensional AFM (3D) case in references [19, 21]. At  $\gamma = 0$ , the above equations would be identical to those of the isotropic two-dimensional (2D) case [18, 19]. At a temperature above  $T_N$ , by virtue of the constraints  $M = 0$  and  $J\gamma = J = \text{const.}$ , Eqs. (15)-(17) are sufficient to determine the three variables,  $\rho$ ,  $\gamma$  and  $\rho$ . At  $T < T_N$ ,  $M$  must be determined. The existence of the Goldstone mode for long range order AFM phase requires  $\rho + \gamma = 1$ , hence there are still three variables  $\rho$ ,  $\gamma$ , and  $M$ . In order to treat the singularity of the Bose-Einstein condensation at  $k = 0$ , we follow reference [18] to use the density of state function

$$\begin{aligned} \rho(x; x^0) &= \frac{2}{N} \sum_k \delta(x - \epsilon_k) \delta(x^0 - \epsilon_k^0) \\ &= \frac{2}{\sqrt{4}^2} K \left( \frac{\rho}{1 + x^2} \right) \frac{1}{\sqrt{4}^2} \frac{1}{1 + x^0^2}; \end{aligned} \tag{18}$$

Therefore,  $f(0)$ ,  $g(\pm)$ , and  $g_z(\pm_z)$  in Eqs. (15), (16), and (17) are rewritten as

$$f(0) = \prod_{i=1}^{Z-1} \prod_{i=1}^{Z-1} dx dx^0! (x; x^0) \prod_{i=1}^{Z-1} \frac{1}{(\tilde{x} + \tilde{\gamma} x^0)^2} \frac{1}{2} \coth \frac{\mu}{2T} \prod_{i=1}^{Z-1} \prod_{i=1}^{Z-1} \quad (19)$$

$$g(\pm) = \prod_{i=1}^{Z-1} \prod_{i=1}^{Z-1} dx dx^0! (x; x^0) \prod_{i=1}^{Z-1} \frac{\tilde{x} + \tilde{\gamma} x^0}{(\tilde{x} + \tilde{\gamma} x^0)^2} \frac{x}{2} \coth \frac{\mu}{2T} \prod_{i=1}^{Z-1} \prod_{i=1}^{Z-1} \quad (20)$$

$$g_z(\pm_z) = \prod_{i=1}^{Z-1} \prod_{i=1}^{Z-1} dx dx^0! (x; x^0) \prod_{i=1}^{Z-1} \frac{\tilde{x} + \tilde{\gamma} x^0}{(\tilde{x} + \tilde{\gamma} x^0)^2} \frac{x^0}{2} \coth \frac{\mu}{2T} \prod_{i=1}^{Z-1} \prod_{i=1}^{Z-1} \quad (21)$$

Then the free energy per site is obtained

$$\frac{F}{N} = i \frac{\mu}{2} \frac{\tilde{\gamma}^2}{ZJ} + \frac{\tilde{\gamma}^2}{Z\tilde{\gamma}J\tilde{\gamma}} \prod_{i=1}^{Z-1} \prod_{i=1}^{Z-1} + \frac{2T}{N} \sum_k \mathfrak{N}_k \ln(\mathfrak{N}_k + 1) - \sum_k \mathfrak{N}_k \ln \mathfrak{N}_k; \quad (22)$$

where  $\mathfrak{N}_k$  is the Bose-Einstein distribution function. The intra-plane and the inter-plane correlation functions are written as

$$\begin{aligned} \langle S_{li} \zeta S_{l;i+\pm} \rangle &= \hat{A}^2 = [M + g(\pm)]^2; \\ \langle S_{li} \zeta S_{l+\pm z;i} \rangle &= \hat{A}_{\tilde{\gamma}}^2 = [M + g(\pm_z)]^2; \end{aligned} \quad (23)$$

From Eq. (22), the specific heat  $C_m$  can be calculated

$$C_m = i T \frac{\partial^2}{\partial T^2} \frac{\mu}{N} F \prod_{i=1}^{Z-1} \prod_{i=1}^{Z-1} \quad (24)$$

## II-2. Numerical results

The numerical results for the free energy, nearest-neighbor correlation function, sublattice magnetization, and specific heat obtained by the MSWT are exhibited in Figs. 1-4. Let's first examine Fig. 1(a) for  $S = 1=2$ . Given a fixed value of  $J_{\tilde{\gamma}}=J$  depending on the temperature there are two lowest energy solutions for Eqs. (19)-(21). One solution, denoted as  $f_0$ , has  $M = 0$ ,  $\tilde{\gamma} = 0$ , and  $\tilde{\gamma} = 0$ ; here the spins are completely uncorrelated. This state has no energy but only a temperature independent entropy. Above a certain temperature  $f_0$  becomes the lowest free energy solution. The other low temperature solution has a finite sublattice magnetization  $M$  and finite spin correlations  $\hat{A}$  as shown in Fig. 2. Results for a series of values of  $J_{\tilde{\gamma}}=J$  are plotted. For  $J_{\tilde{\gamma}} = 0$ , the two-dimensional result as denoted by 2D in Fig. (1) has  $M = 0$  and  $\tilde{\gamma} = 0$ . In the inset of Fig. 1(a), point A denotes the temperature  $T_A = 0.91J$  [18] above which the completely uncorrelated solution  $f_0$  has lower free energy than the 2D result. Point C ( $T_C$ ) in the inset is the crossover temperature for  $f_0$  and the isotropic three-dimensional result with  $J_{\tilde{\gamma}} = J$ . Clearly for values of  $J_{\tilde{\gamma}} = J$  between 0 and 1, the finite  $M$  solution becomes unstable whenever it meets the  $f_0$  solution at a temperature somewhere between  $T_A$  and  $T_C$ . Hence the theory breaks down near and above the crossover temperature. Since the sublattice magnetization  $M$  is finite at the crossover temperature, thus before we reach the Néel temperature, the theory already produces

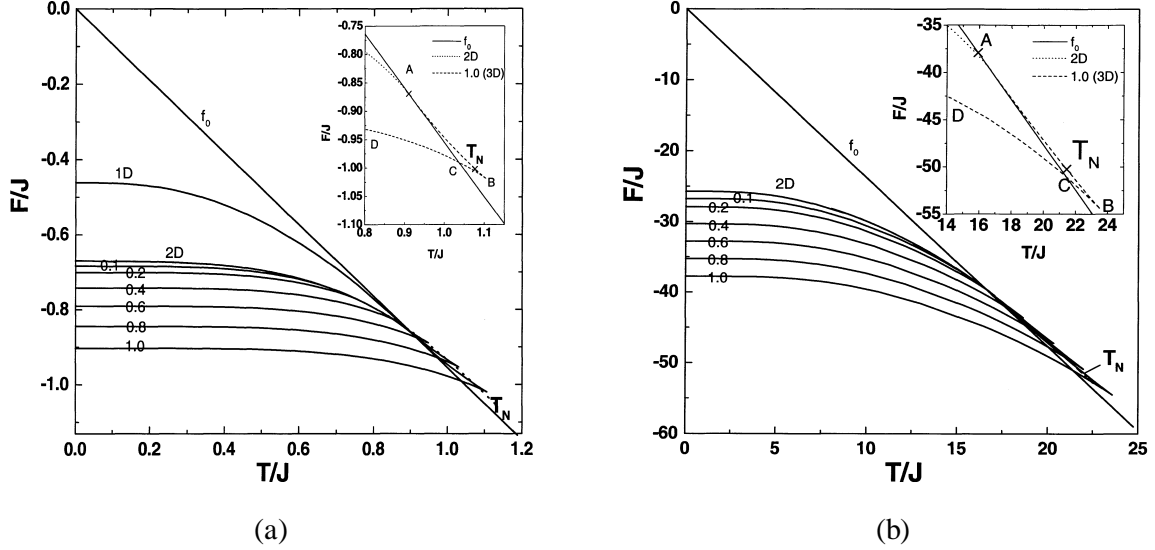


FIG. 1. Free energy as a function of temperature for (a)  $S = 1/2$  and (b)  $S = 7/2$ . The curve  $f_0$  is defined by  $(\zeta = 0; \zeta_\gamma = 0)$ , 1D by  $(\zeta = 0; \zeta_\gamma)$ , 2D by  $(\zeta; \zeta_\gamma = 0)$ . The remaining curves, denoted by  $(J_\gamma = J = )$  0.1, 0.2, 0.4, 0.6, 0.8, 1.0 with specified  $(\zeta; \zeta_\gamma)$ , depict the anisotropic layer antiferromagnet, respectively. The inset of each panel depicts the selected portion of the curves  $f_0$ , 2D and  $J_\gamma = J = 1.0$  about  $T_N$ . The points B, C, D denote the states still preserving the sublattice magnetism. At point A the 2D solution is replaced by the unphysical solution  $f_0$ .

unphysical results. The unphysical nature of the solutions is also reflected in having two solutions of  $g + M$  in Fig. 2(a),  $g_z + M$  in Fig. 2(b) and  $M$  in Fig. 3(a) at a given temperature.

In Fig. 4(a) the ratio of specific heat to temperature  $C_m(T) = T$  is plotted as a function of  $T$  for  $J_\gamma = J = 0.1, 0.6, \text{ and } 1.0$ . Notice that above  $T_C$ , the completely uncorrelated state which has constant entropy has the lowest free energy. Thus there is no specific heat.

Figs. 1(b), 2(c), 2(d), 3(b), and 4(b) are for larger spin  $S = 7/2$ . The results are quite similar to  $S = 1/2$ , except for the low temperature  $C_m(T) = T$ . There is a pronounced shoulder or anomaly for  $S = 7/2$  shown in Fig. 4(b) in comparison with Fig. 4(a). This anomaly is also larger for smaller  $J_\gamma = J$ . Since the smaller the value of  $J_\gamma = J$ , the closer the system approaches two dimensions and the quantum fluctuations are larger. Hence the anomaly is due to the large spin and strong quantum fluctuations. Before we fit the experimental data in Ref. [11] for  $\text{Gd}^{3+}$ , we shall also examine the result in the presence of the magnetic field.

### III. In the presence of a magnetic field

#### III-1. Formalism

In the presence of a magnetic field, magnetizations in the A and B sublattices have different magnitude. Thus  $\langle a_i^y a_i^z \rangle \neq \langle b_m^y b_m^z \rangle$ . This makes the Hamiltonian (Eq. (9)) no longer Hermitian from the mean field approximation of the MSWT. We have attempted to add complex conjugate

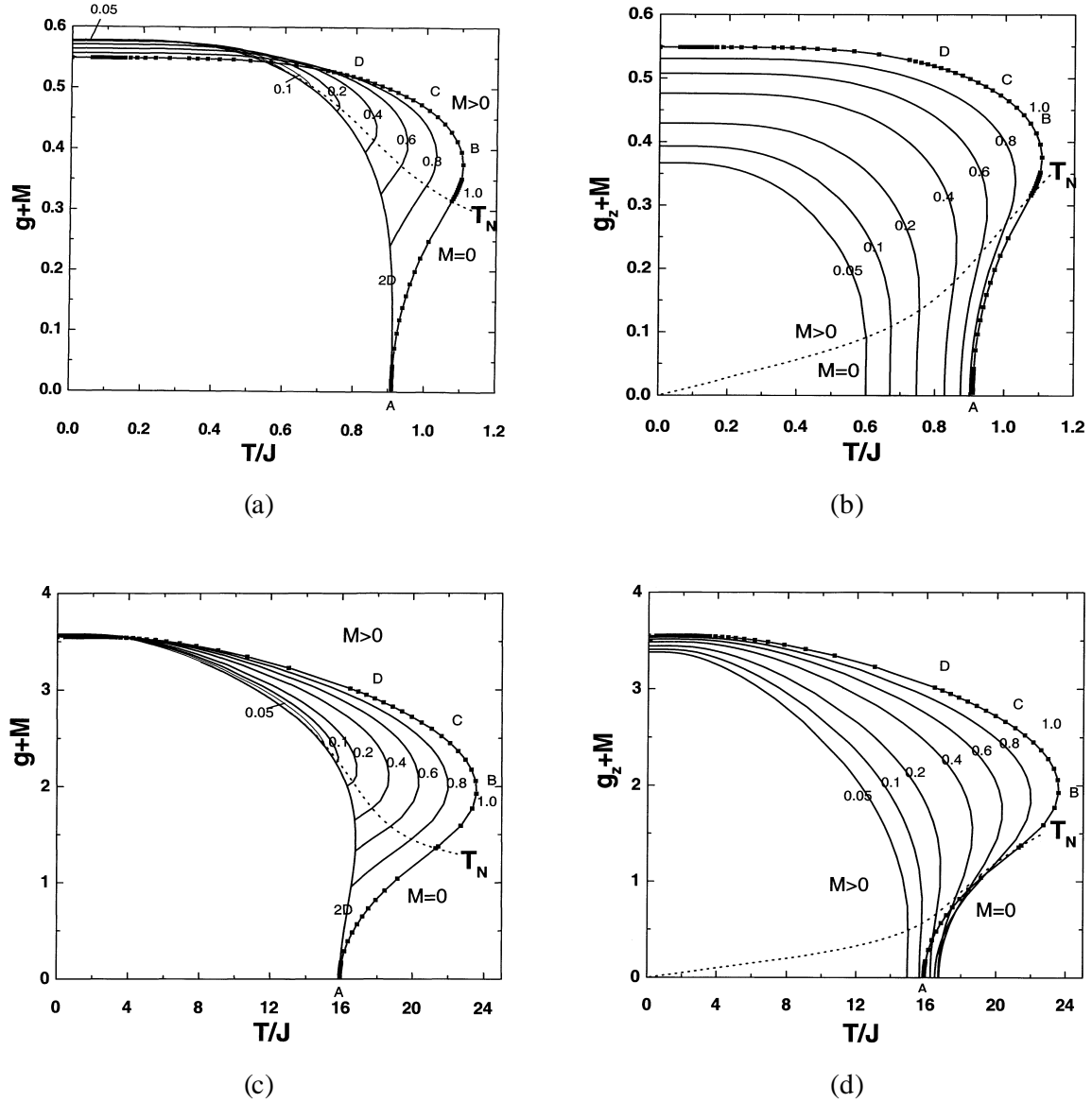


FIG. 2. (a) Intraplane and (b) inter-plane correlations plotted for  $S = 1/2$  for each different value of  $J_z/J$ . (c) and (d) are for  $S = 7/2$ . The dispersion of the result  $T_N$  can be read off from the intersection points of the dotted line and the curves. Here the points A, B, C, and D are same as in Figure 1.

terms by hand to fix this non-Hermitian problem. Nevertheless, we do not obtain any good physical result. Hence the MSWT is abandoned for the work in the presence of an external magnetic field. Instead, we consider the paramagnetic state in which the magnetic field is strong enough to quench the antiferromagnetic long-range order. Hence we use the Holstein-Primakoff (HP) [29]

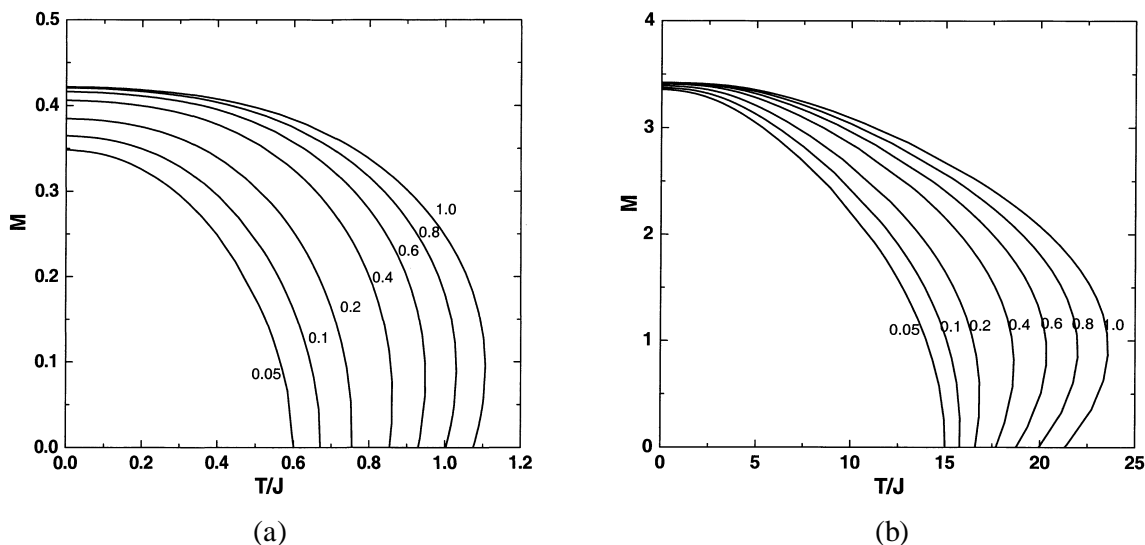


FIG. 3. Sublattice magnetization plotted as a function of temperature for (a)  $S = 1/2$  and (b)  $S = 7/2$  for several values of  $J_z = J$ .

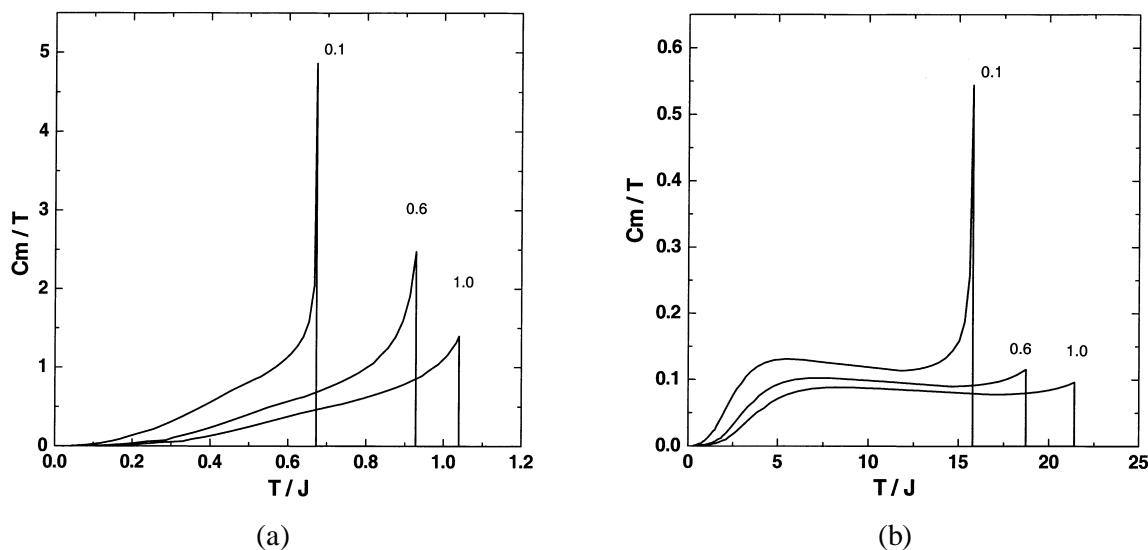


FIG. 4.  $C_m = T$  plotted as function of  $T = J$  for (a)  $S = 1/2$  and (b)  $S = 7/2$  for several values of  $J_z = J$ .

transformation to make a large  $S$  expansion at low temperature. Due to the failure of MSWT to produce reliable results above  $T_N$ , we use a high temperature expansion to estimate the specific heat above  $T_N$ . Besides, we make an extrapolation to low temperatures by using the high temperature expansion.

### III-1-1. Large S expansion

In the presence of a magnetic field, the Hamiltonian is written as

$$H = J \sum_{\langle i,j \rangle} S_{li} S_{lj} + J_z \sum_{i,j} S_{li} S_{l+1,i} + g^1_B H \sum_{li} S^z_{li}; \quad (25)$$

where  $g$  is the Landé  $g$ -factor and  $^1_B$  is Bohr magneton. Assuming the field is strong enough to destroy the AFM, the spin operators on each site can be transferred by the HP transformation

$$\begin{aligned} \hat{S}_{li}^+ &= \rho \frac{\mu}{2S} \sum_{i,j} \frac{a_{li}^y a_{lj}}{2S} a_{li}; \\ \hat{S}_{li}^- &= \rho \frac{\mu}{2S} \sum_{i,j} \frac{a_{li}^y a_{lj}}{2S} a_{li}; \\ \hat{S}_{li}^z &= S - a_{li}^y a_{li}; \end{aligned}$$

To assume the spin to be so large, the approximation of the expansion to order of  $1/S$  is given as

$$\begin{aligned} \hat{S}_{li}^+ &\approx \rho \frac{\mu}{2S} \sum_{i,j} \frac{a_{li}^y a_{lj}}{4S} a_{li}; \\ \hat{S}_{li}^- &\approx \rho \frac{\mu}{2S} \sum_{i,j} \frac{a_{li}^y a_{lj}}{4S} a_{li}; \end{aligned}$$

The Hamiltonian Eq. (25) is approximated as [30, 31]

$$H = \frac{1}{2} (J_z + J_z J_z) N S^2 + \sum_{i,j} [S(a_i^y a_j + a_{i\pm}^y a_{j\pm}) + 2S(a_i a_{i\pm}^y)] + g^1_B H \sum_i (S - a_i^y a_i); \quad (26)$$

Eq. (25) can be diagonalized as

$$H = \frac{1}{2} (J_z + J_z J_z) N S^2 + g^1_B H N S + \sum_k \epsilon_k a_k^y a_k; \quad (27)$$

The energy dispersion, energy per site and the specific heat of bosons are obtained

$$\begin{aligned} \epsilon_k &= J_z S (1 - \cos k) + J_z J_z S (1 - \cos^2 k) + g^1_B H; \\ E &= \sum_{k=N} \epsilon_k; \\ C_m &= \frac{\partial E}{\partial T}; \end{aligned} \quad (28)$$

where  $N$  is the number of sites.

### III-1-2. High temperature series expansion

The Hamiltonian for the high temperature expansion of an antiferromagnet can be treated as in [32, 33]

$$\begin{aligned} H &= H_0 + H_1; \\ H_0 &= \sum_i g^1_B H^X S^Z_{li}; \\ H_1 &= J \sum_{\langle i,j \rangle} S_{li}^X S_{lj}^X + J_\gamma \sum_{\langle i,i+1 \rangle} S_{li}^X S_{i+1,i}^X; \end{aligned}$$

The logarithm of the partition function can be expressed as a series

$$\begin{aligned} \ln Z &= \ln Z_0 + \frac{1}{T} \langle H_1 \rangle_0 + \frac{1}{2!} \langle H_1^2 \rangle_0 - \frac{1}{2} \langle H_1 \rangle_0^2 + \dots \\ &+ \frac{1}{r!} \langle H_1^r \rangle_0 - \dots; \\ Z_0 &= \text{Tr}[\exp(i H_0)]; \\ \langle H_1^n \rangle_0 &= \frac{\text{Tr}[H_1^n \exp(i H_0)]}{Z_0}, \\ & \quad \beta = 1/k_B T; \end{aligned} \quad (29)$$

The specific heat can be derived from the logarithm of the partition function

$$C_V = k_B T^2 \frac{\partial^2}{\partial T^2} (\ln Z); \quad (30)$$

In the present work,  $C_V/T$  is calculated up to terms of the fifth order of inverse temperature as

$$C_V/T \approx C_V^{(1)}(T)/T^3 + C_V^{(2)}(T)/T^4 + C_V^{(3)}(T)/T^5 + \dots; \quad (31)$$

### III-2. Comparison between numerical results and experimental measurements

In Fig. 5, the comparisons between numerical work for the layer antiferromagnet with  $S = 7/2$  and experimental measurements on  $\text{GdBa}_2\text{Cu}_4\text{O}_8$  [11] are shown. In Fig. 5(a), we adjusted both parameters  $J_\gamma = J$  and  $J$  to fit the specific heat anomaly at  $T = 1\text{K}$  on  $\text{GdBa}_2\text{Cu}_4\text{O}_8$  [11]. The best values are  $J = 185\text{ mK}$  and  $J_\gamma = J = 0.05$ . So far there is no direct measurement to determine the values of  $J$  and  $J_\gamma$  for  $\text{GdBa}_2\text{Cu}_4\text{O}_8$ . Our work provides a good estimate for them. In the electron-spin resonance experiments, the intra-plane isotopic exchange integral was estimated to be  $181\text{ mK}$  for  $\text{GdBa}_2\text{Cu}_3\text{O}_y$  [34] and  $156\text{ mK}$  for  $\text{Gd}_{0.01}\text{Y}_{0.99}\text{Ba}_2\text{Cu}_3\text{O}_6$  [17], respectively. The measured anisotropic interaction energy is  $51.7\text{ mK}$  for  $\text{Gd}_{0.01}\text{Y}_{0.99}\text{Ba}_2\text{Cu}_3\text{O}_6$  [17]. This is determined mainly from the contribution of the dipolar interaction. Hence, our results are quite consistent with the above measurements. Our value of  $T_N \approx 2.82\text{ K}$  is somewhat

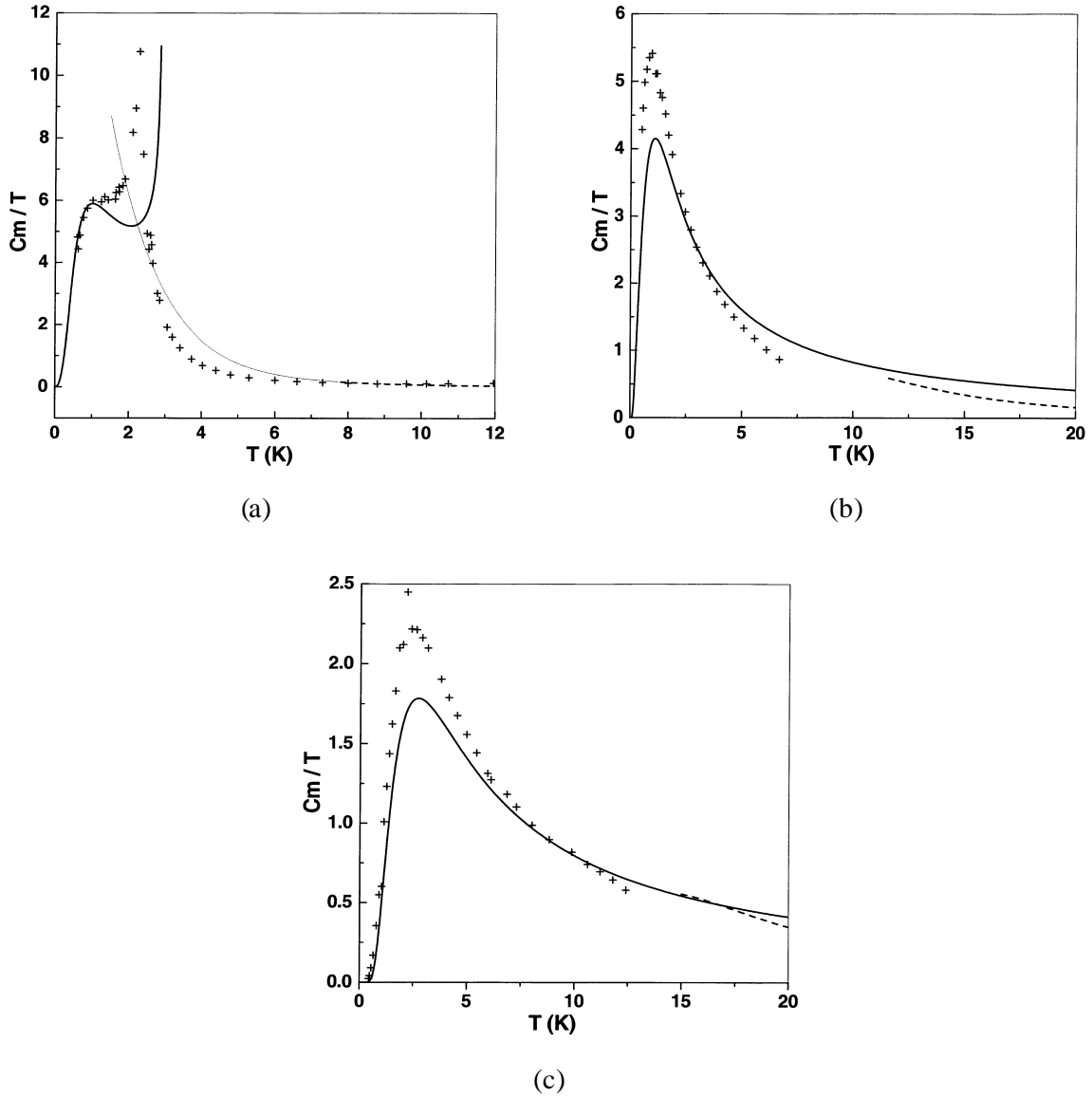


FIG. 5. The  $C_m/T$  plotted as a function of  $T$  for our fitted result and the experimental measurements on  $GdBa_2Cu_4O_8$  [11] for external magnetic fields (a)  $H = 0$  Tesla, (b)  $H = 4$  Tesla and (c) 7 Tesla. In (a), the solid line is the result of the MSWT. In (b) and (c), the solid lines are the results of the large-S expansion. The dashed line gives the high temperature expansion results and the small cross symbols are the experimental data. In (a) the dotted line in the low temperature regime is the extrapolation of the high temperature expansion result. The curves for the high temperature expansion results are truncated at the temperature such that the highest order term  $C_V^{(3)}=T$  contributes about twenty (ten) percent of the total value in panel (a) ((b) and (c)). The fitting parameters are  $J = 0.185$  K and  $J_\gamma = J = 0.05$ .

larger than that of the experimental measured value  $T_N \approx 2.27$  K. Notice that MSWT breaks down before the Néel temperature  $T_N$  is reached. Hence our estimate of  $T_N$  is unreliable. To get some feeling about the result above  $T_N$ , the dashed line is the result of the high temperature expansion method. The dotted line is the extrapolation result.

The numerical results in the presence of external magnetic fields  $H = 4, 7$  Tesla are exhibited in Figs. 5(b) and (c) respectively. We assumed that the  $Gd^{3+}$  layers have no AFM long range order at  $H$  greater than 4 Tesla. Our numerical results agree very well with the experimental measurements at low temperatures.

### III. Conclusions

The specific anomaly observed in experiments [1-15] is explained by a usual Heisenberg model with a layer structure. The experimental observed disappearance of the specific anomaly in the presence of a high external field [11] is also reproduced. Comparison between the result for  $S = 1/2$  and that for  $S = 7/2$  shows that the specific anomaly is due to the large spin of  $Gd^{3+}$  ion. We notice that the anomaly seems to be more pronounced for small  $J_{\parallel} = J$ . Hence the quantum fluctuation also plays a role. The in-plane exchange coupling constant we obtained is close to the experimental value [17, 34] and so is the value of inter-layer exchange coupling constant.

For the isotropic 2D antiferromagnet, the MSWT is quite successful at low temperatures. Although there is also an unphysical solution at high temperatures, it is of no physical relevance. However for the 3D anisotropic layer, this unphysical behavior obtained in the MSWT occurs at temperatures below the Néel temperature  $T_N$ . To avoid the complication arising from the breakdown of the MSWT, we use different methods to understand the properties of the anisotropic layer AFM at low and high temperatures. To use a single method to describe the properties for all temperatures is quite desirable and is left for future work.

### References

- [ 1 ] S. E. Brown *et al.*, Phys. Rev., **B 36**, 2298 (1987).
- [ 2 ] S. Simizu *et al.*, Phys. Rev., **B 36**, 7129 (1987).
- [ 3 ] B. D. Dunlap *et al.*, Phys. Rev., **B 37**, 592 (1988).
- [ 4 ] B. W. Lee *et al.*, Phys. Rev. **B 37**, 2368 (1988).
- [ 5 ] G. H. Hwang *et al.*, Chin. J. Phys. **30**, 351 (1992).
- [ 6 ] Y. Y. Chen *et al.*, Phys. Rev. **B 47**, 12178 (1993).
- [ 7 ] C. C. Lai *et al.*, Phys. Rev. **B 49**, 1499 (1994).
- [ 8 ] J. C. Ho *et al.*, Physica **B 194-196**, 203 (1994).
- [ 9 ] C. L. Yang *et al.*, Physica **B 194-196**, 203 (1994).
- [10] H. L. Tsay *et al.*, Physica, **C 252**, 79 (1995).
- [11] J. C. Ho *et al.*, Physica, **C 282-287**, 1403 (1997).
- [12] M. Bouvier, P. Lethuillier and D. Shmitt, Phys. Rev. **B 43**, 13137 (1991).
- [13] R. Mallik and B. V. Sampathkumaran and references therein, Phys. Rev. **B 58**, 9178 (1998).
- [14] C. Mazumdar *et al.*, Phys. Rev. **B 59**, 4215 (1999).
- [15] N. G. Patil and S. Ramakrishnan, Phys. Rev. **B 59**, 9581 (1999).
- [16] J. A. Blanco, D. Gignoux and D. Schmit, Physical Rev. **B 43**, 13145 (1991).
- [17] F. Simon *et al.*, Phys. Rev. **B 59**, 12072 (1999).

- [18] Minoru Takahasi, Prog. of Theoret. Phys. suppl. **87**, 233 (1986); Phys. Rev. Lett. **58**, 168 (1987); Phys. Rev. **B 40**, 2494 (1989).
- [19] Bang-Gui Liu, J. Phys.: Condens. Matter **4**, 8339 (1992).
- [20] Micheline Bloch, Phys. Rev. Lett. **7**, 286 (1962).
- [21] H. S. Liu, Phys. Rev. **142**, 267 (1966).
- [22] P. D. Loly, J. Phys. **C 1**, 1365 (1971).
- [23] Sanyee Tang, M. E. Lazzouni and J. E. Hirsh, Phys. Rev. **B 40**, 5000 (1989).
- [24] Heinz Barentzen and Piotr Wróbel, Z. Phys. **B 93**, 373 (1994).
- [25] V. Yu. Irkhin, A. A. Katanin and M. I. Katsnelson, The physics of Metals and Metallography, **79**, 42 (1995).
- [26] V. Yu. Irkhin, A. A. Katanin and M. I. Katsnelson, Physical Rev. **B 60**, 1082 (1999).
- [27] F. J. Dyson, Physical Rev. **102**, 1217 (1956), **102**, 1230 (1956).
- [28] S. V. Maleev, Sov. Phys.-JETP **6**, 776 (1958).
- [29] T. Holstein and H. Primakoff, Physical Rev. **58**, 1098 (1940).
- [30] J. Feder and E. Pytte, Physical Rev. **168**, 640 (1968).
- [31] A.F.M. Arts and W. De wijn, in *Spin Waves in Two-Dimensional Magnetic Systems: Theory and Applications*, collected in *Magnetic Properties of Layered Transition Metal Compounds*, ed. L. J. De Jongh (Kluwer, Lodon, Boston and Dordrecht, 1990). J. Feder and E. Pytte, Physical Rev. **168**, 640 (1968).
- [32] C. Domb and M. F. Sykes, Phys. Rev. **128**, 168 (1962).
- [33] C. Domb, *Phase Transitions and Critical Phenomena*, (Academic Press, 1992).
- [34] F. Nakamura *et al.*, Physical Rev. **B 42**, 2558 (1990).